

Computational Study of the Axisymmetric, Supersonic Ejector-Diffuser Systems

Heuy-Dong KIM*, Young-Ki LEE*, Tae-Won SEO* and Srinivasan Raghunathan**

Key Words : Compressible Flow, Supersonic Ejector, Supersonic Nozzle, Internal Flow, Shock wave, Second Throat

Abstract

A ejector system is one of the fluid machinery, which has been mainly used as an exhaust pump or a vacuum pump. The ejector system has often been pointed out to have only a limited efficiency because it is driven by pure shear action and the mixing action between primary and secondary streams. In the present work, numerical simulations were conducted to investigate the effects of the geometry and the mass flow ratio of supersonic ejector-diffuser systems on their mixing performance. A fully implicit finite volume scheme was applied to solve the axisymmetric Navier-Stokes equations, and the standard $k-\epsilon$ turbulence model was used to close the governing equations. The flow fields of the supersonic ejector-diffuser systems were investigated by changing the ejector throat area ratio and the mass flow ratio. The existence of the second throat strongly affected the shock wave structure inside the mixing tube as well as the spreading of the under-expanded jet discharging from the primary nozzle, and served to enhance the mixing performance.

1. Introduction

The ejector system is a device which employs a high-velocity primary motive fluid to entrain and accelerate a slower moving secondary suction fluid. The resulting kinetic energy of the mixture is subsequently used for self-compression to a higher pressure, thus performing the function of a compressor. The ejector system has long been applied to jet pumps, vacuum pumps, high-altitude simulators, V/STOLs, etc⁽¹⁻³⁾, because of the major advantages of its structural simplicity and reliability. However, the ejector system has often been pointed out to have only a limited efficiency in such applications. The defects are mainly because the ejector is derived by the pure shear action and the mixing action between primary and secondary streams, while most of the fluid machinery is operated by the normal stress on the rotating blades. Recently the ejector system is employed to reduce jet exhaust noise⁽⁴⁾ and to enhance air-fuel turbulent mixing in many combustion engines^(5,6), in which the configuration of the ejector influences the whole performance of the system.

Prediction of supersonic ejector flow has been based mainly upon the assumption of one-dimensional compressible flow in both primary and secondary

streams^(7,8). Major weakness of such treatments is that supersonic flows are rarely uniform as assumed, and they are applicable only to systems having constant area mixing tubes ignored viscous mixing effects at the two-stream boundary.

In spite that many unsolved problems still remain, much effort has been devoted towards the improvement of the ejector performance. The enhancement of the turbulent mixing was a main target to achieve such an aim. In doing so, the geometry of the primary nozzle was varied to promote the tangential shear action between the primary and secondary streams. A petal nozzle was a useful means promising a better performance⁽⁹⁻¹¹⁾.

In the present work, the supersonic ejector-diffuser system performing the function as an exhaust pump was investigated using numerical methods. Computations using mass-averaged Navier-Stokes equations were applied to the axisymmetric supersonic ejectors with the second throat and the constant area mixing tube. The governing equations were discretized in space using a fully implicit finite volume differential formulation, based upon fine structured grid system. The standard $k-\epsilon$ turbulence model was employed to close the governing equations. The mass flux of the secondary steam and the cross-sectional area of the second throat were varied to investigate the effects on the mixing performance as well as flow characteristics of the supersonic ejector-diffuser systems.

* Andong National University

** Queen's University of Belfast, UK

2. Navier-Stokes Computations

2.1 Governing Equations

The governing equations are given by the conservation forms of the axisymmetric, mass averaged, time-dependent Navier-Stokes equations. The resulting equations are expressed in an integral form for an arbitrary control volume V ,

$$\Gamma \frac{d}{dt} \int_V \mathbf{Q} dV + \oint [F - G] \cdot dA = 0 \quad (1)$$

where F and G are the inviscid and viscous flux vectors in standard conservation form and Q is the dependent vector of primary variables.

$$\begin{aligned} F &= [\rho v, \rho v v_x + p \hat{i}, \rho v v_y + p \hat{j}, \rho v v_z + p \hat{k}, \rho v H]^T \\ G &= [0, \tau_{xi}, \tau_{yj}, \tau_{zi}, \tau_{ij} v_j + q]^T \\ Q &= [p, v_x, v_y, v_z, T]^T \end{aligned} \quad (2)$$

In Eq.(2), H is total enthalpy per unit mass. The preconditioning matrix Γ is included in Eq.(1) to provide an efficient solution of the present axisymmetric compressible flow⁽¹²⁾. This matrix is given by

$$\Gamma = \begin{bmatrix} \theta & 0 & 0 & 0 & \rho_T \\ \theta v_x & \rho & 0 & 0 & \rho_T v_x \\ \theta v_y & 0 & \rho & 0 & \rho_T v_y \\ \theta v_z & 0 & 0 & \rho & \rho_T v_z \\ \theta H - 1 & \rho v_x & \rho v_y & \rho v_z & \rho_T H + \rho C_p \end{bmatrix} \quad (3)$$

where ρ_T is the derivative of density with respect to temperature at constant pressure and $-p/RT$ for compressible flow. The parameter θ is defined as

$$\theta = (1/U_r^2) - (\rho_T H + \rho C_p) \quad (4)$$

In Eq.(4), the reference velocity U_r is chosen such that the eigenvalues of the system remain well conditioned with respect to the convective and diffusive timescales, and C_p is the specific heat at constant pressure.

Two-equation, standard k - ϵ model, which is modified to take account for compressibility effect, is employed to close the governing equations. The turbulent model for μ_t is written by $\mu_t = \rho C_\mu (k^2/\epsilon)$, where the turbulent kinetic energy k and dissipation rate ϵ are solved from the turbulent transport theory. The standard model constants are used:

$$C_\mu = 0.09, C_{1\epsilon} = 1.44, C_{2\epsilon} = 1.92, \sigma_k = 1.3, \sigma_\epsilon = 1.0$$

2.2 Computational Domain and Grid

The present supersonic ejector-diffuser system with a second throat is composed of the primary stagnation chamber, the primary convergent-divergent nozzle, the secondary flow inlet, and the diffuser, as schematically shown in Figure 1. The primary nozzle and second throat heights are defined as H_p and H_2 , respectively. A

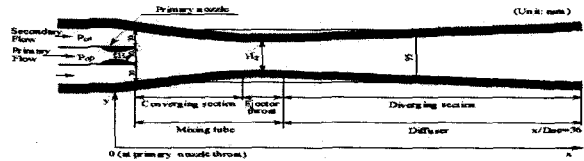


Fig. 1 Supersonic ejector-diffuser flow

convergent-divergent nozzle with a design Mach number of $M_{1p} = 2.11$ was applied to the present computations. The mixing tube of a length of 250mm includes both the converging section of the ejector and the second throat section. A straight channel with a length of 50mm and height of H_2 consists of the second throat of the present ejector-diffuser system, connecting the mixing tube with the diffuser.

The secondary flow inlet is to give a mass influx into the ejector-diffuser system. The ejector throat area ratio Ψ , is defined by H_2/H_p . The total pressures at the primary and secondary flows are defined as p_{0p} and p_{0s} , respectively. The back pressure p_a of the ejector-diffuser system was kept constant by 101.3kPa. The operating pressure ratio, p_{0p}/p_a was kept constant by 10.0 to obtain the supersonic operation of the ejector-diffuser system for different ejector throat area ratios.

The supersonic ejector-diffuser flow is represented on the computational domain of fine structured grids. In the computations about 50,000 grid points were applied to only the upper part on the axis of the ejector-diffuser system.

2.3 CFD Scheme and Boundary Conditions

The governing equations aforementioned are discretized spatially using a fully implicit finite volume scheme. Using a second order accurate scheme makes it feasible to capture the shock structure and the boundary layer flows near the ejector walls, but only with fine computational grids there. With respect to temporal discretization, an explicit multi-stage time stepping scheme is used to discretize the time derivatives in the governing equations. Then the solution is advanced from time t to time $t + \Delta t$ with a multi-stage Runge-Kutta scheme.

A convergence criterion of the solutions was established when the residuals for each of the conserved variables have reduced below the order of a magnitude of 3. Another convergence criterion is to directly check the conserved quantities through the computational boundaries. The net mass flux was investigated if there were an applicable imbalance through the computational boundaries.

The pressure inlet boundary condition, which was applied to the inlet boundary of the primary nozzle, facilitates the input of the inflow direction and speed. Total properties of the flow are required with the static pressure at the inlet boundary, specified by an isentropic relation. Mass influx boundary condition was applied to

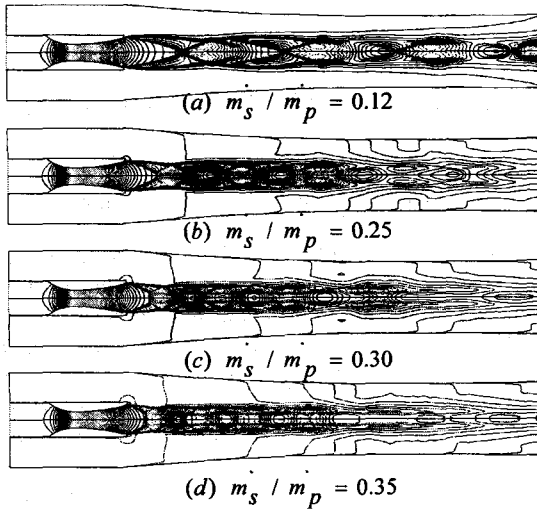


Fig.2 Isopycnics for various m_s / m_p values ($\psi=4.39$ and $p_{op} / p_a=10$)

the secondary flow inlet. The pressure outlet condition for the exit boundary of the ejector-diffuser system requires only a static pressure specification for locally subsonic flow. If the flow is supersonic at the outlet boundary then the pressure is extrapolated from the interior with all other flow variables always being extrapolated regardless of local pressure fluctuations because of a hyperbolic nature of the supersonic flow.

3. Results and Discussion

To investigate the mixing performance of supersonic ejector-diffuser systems, the ejector throat area ratio ψ and the secondary mass flow were changed for the fixed values of the operating pressure, $p_{op}/p_a=10$ and the design Mach number of the primary nozzle, $M_{1p}=2.11$.

Figure 2 shows the isopycnics for various mass flow ratios. In the Figure 2(a), the primary stream accelerates to a supersonic speed through the convergent-divergent nozzle, resulting in an over-expanded jet at the exit of the primary nozzle. The first oblique shock wave, which appears at the nozzle exit, reflects on the axis of the ejector-diffuser system and forms a strong shock wave, consequently leading to deceleration of the primary supersonic flow.

As the secondary mass flow rate increases, the oblique shock wave forms Mach disk so that the primary flow near ejector axis undergoes more intense deceleration. Reflections of the oblique shock result in a multiple of oblique shock system⁽¹³⁾. Downstream of the nozzle exit, the supersonic flow past the Mach disk and the subsonic flow past the oblique shock has the same temperature and pressure but different velocities. This boundary called a slip line leads to a strong shear action.

Figure 3 is present isopycnics of the ejector-diffuser systems having a small ψ value, 3.70. For the same mass

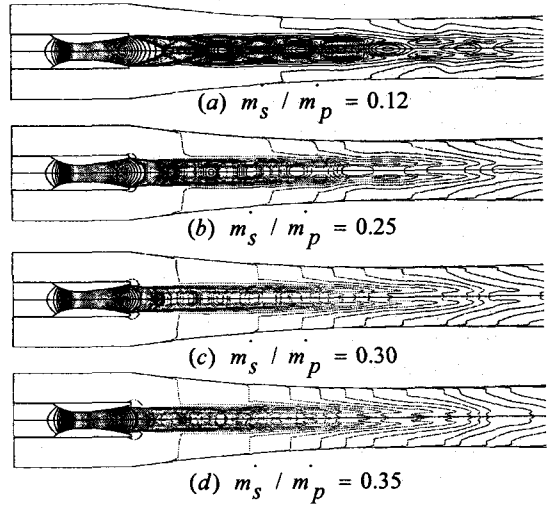


Fig.3 Isopycnics for various m_s / m_p values ($\psi=3.70$ and $p_{op} / p_a=10$)

flow ratio shown in Figure 2 and Figure 3, there seems to be a notable difference the structures of two primary streams. For instance, in the Figure 3(a) the oblique shock reflects on the axis of the ejector-diffuser system to form a Mach disk while the oblique shock seems to be very close to a regular reflection. Furthermore the difference in this shock pattern, there are some differences in the structures of the primary stream boundaries and the locations of the shock systems embedded into the streams. Especially as the mass flow ratio grow up, the position of the first oblique shock wave is located to the inner part of the primary nozzle. This confirms that the mixing of the two streams is dependent on the mass flow ratio as well as the flow configuration.

In order to investigate the effect of the second throat on the flow field of the ejector-diffuser systems and compare flow characteristics for a second throat with those for a constant area mixing duct, Figure 4 shows the isopycnics for various ψ values. As the ejector throat area ratio decreases, the effect of the back pressure imposed at the vicinity of the exit of the primary nozzle appears significant, resulting in the Mach disk to move more upstream and the physics of flow fields significantly to vary. In the present work, flow characteristics of the constant area mixing tube type like Figure 4(a) were not seriously depend on the variation of the mass flow ratio, but those of the constant area mixing tube types like Figure 4(b) and (c) as aforementioned in the Figure 2 and 3. The effect of the second throat leads to stronger shear action and mixing between the primary

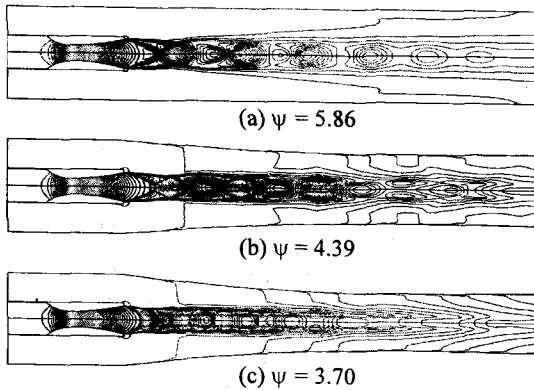


Fig.4 Isopycnics for various ψ values ($m_s/m_p=0.25$, $p_{0p}/p_a=10$)

flow and the secondary flow, consequently resulting in a better exhaust performance.

Figure 5 show the local Mach number distributions along the axis of the ejector-diffuser system. The distance x , its origin being located at the throat of the primary nozzle, is normalized using the height of the primary nozzle exit, D_{ne} . Note that the second throat of the ejector-diffuser systems, as illustrated in Figure 1, is located at the regime of $8.0 < x/D_{ne} < 9.67$.

For the constant area mixing tube of $\psi=5.86$, the local Mach number appears to largely fluctuate on the axis of the ejector-diffuser system. This results from a multiple of shock waves. The fluctuations seem to be limited to the region of $x/D_{ne} < 13$, corresponding to a location downstream of the second throat and the large fluctuations in local Mach number appear inside the mixing tube. The effect of the mass flow ratio on the local Mach numbers seem to be insignificant, except for the data of $m_s/m_p=0.12$. In the region of $x/D_{ne} > 13$ the flow decelerates monotonously up to a subsonic speed at the exit of the diffuser.

Unlike the local Mach number distributions shown in Figure 5(a), Figure 5(b) and (c) show the local Mach numbers for the second throat ejector-diffuser system. In comparison with the results for $\psi=5.86$, the local Mach number fluctuations continue up to more downstream locations, and the peak Mach numbers appear higher. A notable change in the local Mach number is found with different mass flow ratios.

In Figure 5(b), for low mass flow ratios of $m_s/m_p=0.12$ and 0.25 , some weak shock waves are found downstream of the second throat. But for relatively high mass flow ratios the flow accelerates through the diffuser up to local Mach numbers above 2.2, and consequently forming the new shock systems near the diffuser exit. So the flow experiences a double choke at both the primary nozzle throat and the second throat⁽¹⁴⁾. But in Figure 5(c) these phenomena are observed in the entire mass flow ratio. In these cases the mixing of the primary and

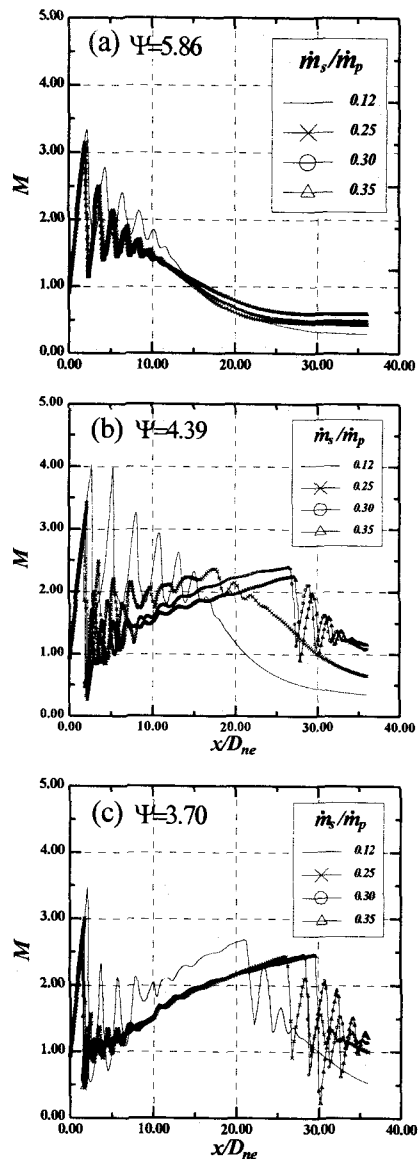


Fig.5 Mach number distributions along the axis for various m_s/m_p values ($p_{0p}/p_a=10$)

secondary flows becomes independent of the pressure variation downstream of the diffuser.

To investigate the mixing performance of the supersonic ejector systems, Figure 6 shows the streamwise static pressures on the axis and along the wall surface with the variation of the throat area ratio. As the ψ values decrease, flow characteristics inside the supersonic ejector flow fields are changed dramatically as aforementioned in Figure 4. In the case of having the constant area mixing tube, $\psi=5.86$, from a comparison of the static pressure distributions on the axis and along the wall of the ejector, it is known that the two static pressures are nearly the same downstream of $x/D_{ne}=12$, indicating uniform flows there.

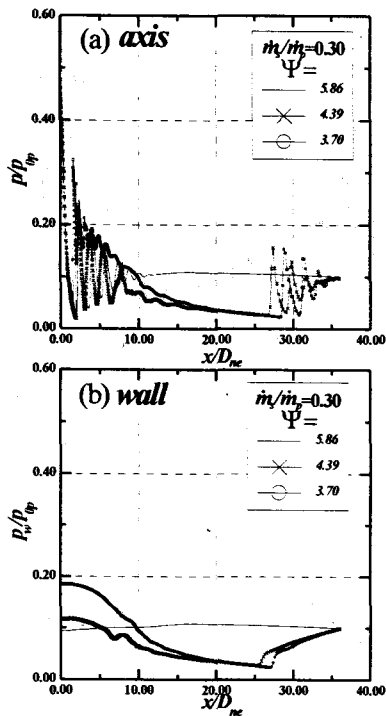


Fig.6 Static pressure distributions for various ψ values ($m_s/m_p=0.30$ and $p_{0p}/p_a=10$) (a) along the axis, (b) along the wall

However, for the ejector-diffuser systems with a second throat, $\psi=4.39$ and 3.70 , two static pressure values are nearly coincide with each other at about $x/D_{ne}=10$ and 8 respectively, indicating the positive effect on the mixing performance of the second throat. As a result, installing the second throat inside the supersonic ejector system ensures more vigorous mixing actions than the case of the constant area mixing tube, leading to improved exhaust performance.

4. Conclusions

In the present work, the supersonic ejector-diffuser systems with a constant area mixing tube and a second throat were computed using axisymmetric compressible Navier-Stokes equations with standard $k-\epsilon$ turbulence model. The mixing performance of the system was investigated by changing the secondary mass flow rate and the ejector throat area ratio. For the constant area mixing tube the secondary mass flow did not significantly change the flow characteristics in the ejector-diffuser systems. However, the flow in the ejector-diffuser systems having the second throat was strongly dependent on the secondary mass flow. It was found that this was due to the effect of the back pressure prevailing at the vicinity of the exit of the primary nozzle. Static pressure distributions on the axis and the walls of the ejector-diffuser systems showed that the ejector-

diffuser systems with the second throat ensure more vigorous mixing actions, compared with the constant area mixing tube, consequently leading to improved exhaust performance

References

- (1) Vogel, R., 1956, "Practical Application of Air Ejectors," NASA TT F-9352.
- (2) Alperin, M. and Wu, J. J., 1983, "Thrust Augmenting Ejectors, Part 2," AIAA Jour., Vol.21, No.12, pp.1698-1706.
- (3) Yang, T. T., Ntone, F., Jiang, T. and Pitts, D. R., 1985, "An Investigation of High Performance, Short Thrust Augmenting Ejectors," Jour. Fluids Eng., Vol.107, pp.23-30.
- (4) Dong, T. Z. and Mankbadi, R. R., 1999, "Simulation of Unsteady Flow in Nozzle-Ejector Mixer," Jour. Propulsion and Power, Vol.15, No.4, pp.539-543.
- (5) Francis, W. E., Hoggarth, M. L. and Templeman, J. J., 1972, "The Design of Jet Pumps and Injectors for Gas Distribution and Combustion Purposes," Proceedings of Symposium on Jet Pumps and Ejectors, BHRA Fluid Engineering-Institution of Chemical Engineers, London, England, No.6, pp.81-96.
- (6) Liu, C. F. and Chen, F., 1992, "Analysis of Performance of The Second-Throat Ejector-Diffuser," Journal Chinese Soc. Mech Engr., Vol.13, No.5, pp.478-482.
- (7) Hsu, C. T., 1972, "Investigation of an Ejector heat Pump by Analytical Methods," ORNL /CON-144, Oak Ridge National Laboratory.
- (8) Quinn, B., 1976, "Ejector Performance at High Temperatures and Pressures," Journal of Aircraft, Vol.13, No.12, pp.948-954.
- (9) Nicholas, T. M. T., Narayanan, A. K. and Muthunayagam, A. E., 1995, "Mixing Pressure Rise Parameter for Effect of Nozzle Geometry in Diffuser-Ejectors," Journal Propulsion and Power, Vol.12, No.2, pp.431-433.
- (10) Srikrishnan, A. R., Kurian, J. and Sriramulu, V., 1996, "An Experimental Study on Mixing Enhancement by Petal Nozzle in Supersonic Flow," Journal of Propulsion and Power, Vol.12, No.1, pp.165-169.
- (11) Yu, S. C. M. and Xu, X. G., 1998, "Confined Coaxial Nozzle Flow with Central Lobed Mixer at Different Velocity Ratios," AIAA Jour., Vol.36, No.3, pp.349-358.
- (12) Weiss, J. M. and Smith, W. A., 1995, "Preconditioning Applied to Variable and Constant Density Flows," AIAA Jour., Vol.33, No.11, pp.2050-2057.
- (13) Kim, H. D., Lee, Y. K. and Seo, T. W., 1999, "A CFD Study of the Supersonic Flows in the Second Throat Ejector-Diffuser Systems," Third International Conference on Fluid Mechanics and Heat Transfer, Dec. 15-16 1999, Dhaka, Bangladesh, pp.348-391.
- (14) Kim, H. D., Setoguchi, T., Yu, S., and Raghunathan, S., 1999, "Navier-Stokes Computations of the Supersonic Ejector-Diffuser System with a Second Throat," Jour. of Thermal Science, Vol.8, No.2, pp.79-88.